A STUDY OF THE DYNAMICS OF AN ORDER-DISORDER PHASE TRANSITION IN Ni_3Mn BY NEUTRON DIFFRACTION

by

GLENN GRIFFIN, B.Sc.

A Thesis
Submitted to the Physics Department
in Partial Fulfilment of the Requirements
for the Degree of
Master of Science

McMaster University
September 1972

ACKNOWLEDGEMENTS

I wish to thank my supervisor Dr. M.F. Collins for suggesting the topic for this research, and Drs. Collins and H.C. Teh for their amiable assistance concerning the technical matters and the theory of this work. The graduate student members and technician of Dr. Brockhouse's group have earned my appreciation for aid in both material and intellectual matters. Without the use of an electric furnace designed and constructed by Mr. S. Boronkay, the work could not have been attempted. Finally I wish to thank the graduate students of the Physics Department for making my stay at McMaster an enjoyable one.

TABLE OF CONTENTS

INTRODUCTION

Order-Disorder

The order-disorder phase transition is a major problem in physics. One of the simplest order-disorder systems to study is that of a binary alloy. For reasons to be discussed later, Ni_3Mn has been chosen for our work. This system has been studied qualitatively by Shull and Siegel (1949).

In order to clarify the characteristics of an order-disorder phase transition let us consider a simple alloy AB. We presume this alloy to be a substitutional solid solution in which an atom A of one constituent substitutes at random for an atom B of the other species on the available sites of the lattice. When the substitution is random the system is denoted as a disordered solid solution. In some systems (including our own) such a structure can be transformed, by suitable heat treatment, into an ordered solid solution in which the A atoms are preferentially located with respect to neighbouring B atoms but are still on the same lattice sites occupied in the disordered states. The A atoms occupy one set of lattice sites while the B atoms occupy another, thereby creating a superlattice structure.

A simple example of the order-disorder effects is shown in Fig. 1 for an AB alloy having equal atomic percentages of the two atoms and crystallizing in a body-centred cubic structure. In the disordered state B atoms have merely substituted at random for A atoms whereas in the ordered state there are discrete planes of A atoms and discrete planes of B atoms.

Geometrical Structure Factor

The crystal lattice of the Ni_3Mn alloy is face-centred cubic and in the ordered phase, has Mn atoms at the cube corners and Ni atoms at the face-centred positions. Kittel (1966) gives the geometrical structure factor for a crystal lattice.

$$S\,(hkl) = \sum_j f_j \exp\left[-i2\pi\,(u_j h + v_j k + w_j l)\right]$$

(where the position of the j^{th} atom within the unit cell is specified by $\underline{r}_j = u_j\underline{a} + v_j\underline{b} + w_j\underline{c}$ where u_j, v_j, w_j are constants. This factor need not be real since the intensity involves S^*S where S^* is the complex conjugate of S. It can be shown that for a lattice with a centre of symmetry S is real.

The basis of the fcc structure referred to the usual cubic unit cell has identical atoms at uvw = 000; $0\frac{1}{2}\frac{1}{2}$; $\frac{1}{2}0\frac{1}{2}$; $\frac{1}{2}\frac{1}{2}0$. For ordered Ni_3Mn, however, we have Mn atoms at 000 and Ni atoms at $0\frac{1}{2}\frac{1}{2}$; $\frac{1}{2}0\frac{1}{2}$, $\frac{1}{2}\frac{1}{2}0$. Thus our geometrical structure factor becomes

$$S\,(hkl) = f_{Mn} + f_{Ni}\left\{\exp[-i\pi\,(k+l)] + \exp[-i\pi\,(h+l)] + \exp[-i\pi\,(h+k)]\right\}$$

If all indices are even integers or if all are odd integers we have

$$\mathbf{S}(hkl) = f_{Mn} + 3f_{Ni}$$

If the indices are not all even or all odd we have

$$\mathbf{S}(hkl) = f_{Mn} - f_{Ni}$$

One of the reasons for selecting the Ni_3Mn system is that the "superlattice" peak intensities are greatly enhanced because of the reversed phase neutron scattering for manganese with reference to that for nickel. The scattering length for manganese is -0.36×10^{-12} cm. and that for nickel is 1.03×10^{-12} cm. Thus $\mathbf{S}_o$ (for Ordinary Reflections) is

$$\begin{aligned}\mathbf{S}_o &= f_{Mn} + f_{Ni}\\ &= (-0.36 + 3 \times 10^{-12} \text{ cm.}\\ &= 2.73 \times 10^{-12} \text{ cm.}\end{aligned}$$

and $\mathbf{S}_s$ (for Superlattice Reflections) is

$$\begin{aligned}\mathbf{S}_s &= f_{Mn} - f_{Ni}\\ &= (-0.36 - 1.03) \times 10^{-12} \text{ cm.}\\ &= -1.39 \times 10^{-12} \text{ cm.}\end{aligned}$$

We recall that intensity is proportional to $\mathbf{S}^*\mathbf{S}$ so that our intensities for ordinary and superlattice reflections will have a ratio of about 4 to 1 ordinary to superlattice judging by geometrical structure factors alone.

Long-Range Order Parameter

The long-range order parameter is easy to measure experimentally and has fundamental significance. According to Guttman (1956) the amplitude of a superlattice reflection is proportional to the difference in atomic scattering factors of the two metals comprising the crystal, to the number of scattering atom and to the long-range order parameter S. Hence the intensity is proportional to the products of the squares of these three variables.

$$I_s = [-N(f_{Mn} - f_{Ni})S]^2$$

where N is the number of Mn atoms.

I_o, the intensity of a fundamental reflection is given by

$$I_o = [N(f_{Mn} + 3f_{Ni})]^2$$

Hence from the ratio $\frac{Is}{Io}$ the order parameter S can be determined.

Extinction

Comparisons are ordinarily made of "integrated intensities", this is, of the areas under curves of intensity against diffraction angle since peak intensities may be sensitive to line shape. We must be sure to account for all effects on our intensities because we hope to extract an order parameter from intensity measurements. We must take into account specifically the extinction properties of the crystal we are working with since it is fairly large.

What is extinction? There are two types - primary and secondary. Primary extinction is the result of attenuation of the incident beam by the process of reflection by successive planes. For neutrons this will occur when the crystal thickness is greater than about 1000 A^{o} (Bacon 1962). We assume, however, that our large single crystal is made up of many small perfect crystals which are misoriented from one to another. It is known from other experimental work that these small perfect crystals have a thickness such that primary extinction is negligible.

This brings us to the topic of secondary extinction. At any particular angular setting of the crystal the beam will eventually reach mosaic blocks (the small perfect crystals) identical in orientation to some of those through which the beam has already passed. In this case the beam may be attenuated by secondary extinction between mosaic blocks.

Assuming a Gaussian distribution of mosaic blocks with standard deviation η, then by a difficult calculation Bacon (1962) derives a criterion for negligible extinction infinite crystal slabs

$$\frac{Qt_o}{\sin\theta\,\eta} < \frac{1}{4}$$

where t_o is the thickness of the crystal; Q the reflectivity; and θ the angle of entrance of the incident beam. The satisfaction of this criterion ensures proportionality of predicted and measured reflectivities to within 5% accuracy. In order to apply this criterion to our own crystal we were forced to make use of a number of gross approximations. Our crystal is cylindrical and is not mounted in the equatorial position but has the cylindrical axis tilted 30° off the vertical. We assume for the calculation that the crystal is a vertically oriented infinite crystal slab. Also, the evaluation of η, the mosaic spread parameter is somewhat difficult so we have assumed a value of $\eta = 25'$ for our crystal (since our narrowest measured Bragg peak has a full width at half maximum of 1.1 degrees). We replace $\frac{to}{\sin\theta}$ by D = 1.6 cm., the diameter of our crystal and calculated Q for the (200) plane where

$$Q = \frac{\lambda^3 N_i^2}{\sin 2\theta} F^2$$

where λ is neutron wavelength, Ni is the number of unit cells per unit volume, F is the structure factor and θ is the Bragg angle for the appropriate plane. Bacon defines the structure factor

$$F = \left| \sum_j f_j \exp[-i2\pi(u_j h + v_j k + w_j l)] \right|^2 e^{-2W}$$

(in our notation) which is the same as our geometrical structure factor except for the term e^{-2W}, the Debye-Waller factor, which takes into account the effect of thermal vibrations.

We have already calculated the geometrical structure factor and we know λ, θ and Ni. This leaves only e^{-2W} to be evaluated. This factor arises in standard phonon theory and describes the temperature dependence of Bragg reflections in terms of the Debye model for a solid.

$$W = B \left(\frac{\sin \theta}{\lambda}\right)^2$$

where $\left(\frac{\sin \theta}{\lambda}\right)$ contains the (hkl) planar dependence of the factor.

$$\frac{\sin \theta}{\lambda} = \frac{1}{2d}$$

For (200) plane for Ni_3Mn ($a = 3.58 \times 10^{-8}$ cm.)

$$\frac{\sin \theta}{\lambda} = \frac{1}{3.58 \times 10^{-8} \text{ cm.}}$$

Now we consider the temperature dependent factor

$$B = \frac{6h^2}{M_a k \Theta} \left\{ \frac{\varphi(x)}{x} + \frac{1}{4} \right\}$$

where $\frac{1}{4}$ accounts for zero-point motion;

$$\varphi(x) = \frac{1}{x} \int_0^x \frac{\xi}{e^\xi - 1} d\xi$$

is the Debye phonon density of states term;

$$x = \frac{\Theta}{T} \simeq \frac{400^\circ}{300^\circ}$$

if Θ is the average Debye Temperature in degrees Kelvin; T is the temperature at which the measurement is taken; Ma is the weighted average mass of the atoms involved, h is Planck's constant and k is the Boltzmann constant. We use the cgs system of units. We thus find

$$B = 39.03 \times 10^{-18} \text{ cm.}^2$$

Hence for the 200 plane

$$e^{-ZW} = e^{-2B\left(\frac{\sin\theta}{\lambda}\right)^2}$$

$$= 0.939$$

Thus the reflectivity for the (200) plane is

$$Q = \frac{\lambda^3 N_i^2}{\sin 2\theta} F^2$$

$$= 0.737 \times 10^{-2} \times 0.939 \text{ cm.}^{-1}$$

$$= 0.692 \times 10^{-2} \text{ cm.}^{-1}$$

Now

$$\frac{Qt_0}{\eta \sin\theta} = \frac{QD}{\eta}$$

$$= \frac{0.692 \times 10^{-2} \text{cm.}^{-1} \times 1.6 \text{cm.}}{25 \times \frac{\pi}{180} \times \frac{1}{60}}$$

$$\simeq \frac{.692 \times 10^{-2} \times 1.6 \times 300}{2}$$

$$\simeq 1.66$$

This is greater than $\frac{1}{4}$ so Bacon's criterion for negligible extinction is not valid for our crystal and in order to make it valid we would have to reduce crystal thickness by a factor of about 6.

Walter C. Hamilton (1957) discusses secondary extinction in cylindrical single crystals. More particularly he gives approximate values for a secondary extinction correction E_s, with sufficient conditions for certain error limits (2% or 5% error).

We again employed some rough approximations in order to compare the actual conditions of our crystal with those sufficient to give an extinction correction error comparable to our statistical error associated with neutron intensity measurements.

Hamilton bases his error conditions on a factor σD where D is the crystal diameter (assuming that the crystal is oriented for an equatorial reflection - which ours approximates) and $\sigma = Q' W(\Delta\theta)$ where Q' is the reflectivity corrected for primary extinction (which we ignore) and $W(\Delta\theta)$ is the distribution function for mosaic blocks in terms of $\Delta\theta$, the deviation of a mosaic block from the mean Bragg angle θ. It is generally assumed that $W(\Delta\theta)$ is a Gaussian distribution function with standard deviation η, termed the mosaic spread parameter. However, it will be convenient here to follow Hamilton's example and to adapt a simpler form for $W(\Delta\theta)$ as follows:

$$W(\Delta\theta) = \begin{cases} \frac{1}{2\eta\sqrt{3}} & \text{if } |\Delta\theta| \le \eta\sqrt{3} \\ 0 & \text{if } |\Delta\theta| > \eta\sqrt{3} \end{cases}$$

This step is justified in the appendix of Hamilton's paper.

Let us now calculate σD for the (200) reflection from our crystal of Ni_3Mn. We assume $\eta \simeq 25'$.

$$
\begin{aligned}
\sigma D &= Q\, W(\Delta\theta)\, D \\
&= \frac{\lambda^3 N i^2}{\sin 2\theta} F^2 \frac{1}{2\eta\sqrt{3}} D \\
&\simeq 0.692 \times 10^{-2}\,\mathrm{cm}^{-1} \times \left(\frac{1}{2 \times \frac{25}{60} \times \frac{1}{60} \times \sqrt{3}}\right) \times 1.6\,\mathrm{cm}. \\
&\simeq 0.47
\end{aligned}
$$

This value for σD satisfies Hamilton's conditions for less than 5% error when using a secondary extinction correction of the form

$$E_s = \exp(-8\sigma D/3\pi)$$

We have also assumed for the above calculation a negligible absorption term for our crystal and that 2θ, the scattering angle, is 0°. The accuracy obtainable according to Hamilton is comparable with our other statistical errors. If necessary, higher order reflections with lower reflectivity may be used in order to decrease the effects of extinction. It appears therefore that extinction can be satisfactorily corrected for in this experiment.

Ising System

We must now connect the eventual results of this experiment with the appropriate theoretical background and predictions.

It can be shown (Huang, 1963) that the order-disorder process in a binary alloy is able to be represented theoretically by the Ising Model whose Hamiltonian is generally given by

$$\mathcal{H} = \sum_{j} J_{ij}\sigma_i\sigma_j$$

In our particular system σ_i , the Ising spin variable takes a value ± 1 according to whether a lattice site is occupied by an Ni atom or an Mn atom. It is assumed that $J_{ij} = V$ if i and j are nearest neighbours and $J_{ij} = 0$ otherwise.

This model has not been solved exactly in 3- dimensions, even though the spin dimensionality is only 1. The 3-dimensional Ising model results which have been obtained, were developed through the use of series expansions, Padé approximant method and other techniques.

Our interest lies in the dynamical aspect of the order-disorder phase transition. Some theoretical work (but no experimental work) has been done in this area. A theoretical study of a 2- dimensional Ising model using the method of computer simulation has been done by Ogita, Ueda, Matsubara Matsuda and Yonezawa (1969).

The authors have simplified a 3- dimensional lattice model to a 2- dimensional model projected onto a plane perpendicular to the c- axis of the crystal. Necessary parameters such as temperature, external field etc. are given as input data for the computer simulation. The ordered configuration is stored as an initial state, then a bond is chosen by a random number. The computer observes the spin values corresponding to the chosen bond and its six neighbours. It finds the transition probability for the observed configuration, (which is assumed proportional to the Boltzmann factor for the activation energy) and compares this probability with another random number between 0 and 1. If the probability is larger than the random number, the sign of the spin variable is changed. After this process is repeated 2^{15} times, a unit time is considered to have passed. Then, polarization, spin correlation and the pattern of the spin configuration at that time are output. The whole procedure is repeated until the system attains an equilibrium state.

The most interesting result is contained in a log-log plot of the relaxation time of polarization versus $(T-T_c)/T_c$. The graphical points are joined very closely by a straight line with gradient $-7/4$ which agrees very well with the value of the critical exponent of susceptibility obtained by the Padé approximation.

Yahata (1971) has used a Markoffian stochastic model of interacting Ising spins to study the long-time behaviour of relaxation of its magnetization and energy near T_c. The technique of high-temperature series expansion and the ratio method are employed in this investigation. A numerical estimate is made of the critical exponent Δ_{MM} of slowing down of magnetization. For a 3-dimensional Ising model the exponent is predicted to be $\Delta_{MM} \simeq 1.4$. The paper also shows the possibility that the critical exponent of slowing down of magnetization is different from that of static susceptibility, contrary to the estimate from the initial decay or the result which the molecular field theory gives.

Magnetization, for a ferromagnet corresponds to long range order in a binary alloy such as Ni_3Mn. Thus we can compare our experimental measurements of long range order with the theoretical predictions for magnetization.

APPARATUS

Our source of monochromatic neutrons is the two-axis spectrometer associated with the McMaster University reactor. The spectrometer consists of a monochromator, a specimen table (which can be rotated) and a helium-3 neutron counter with associated electronics. (See Fig.3) The monochromator is an aluminum single crystal oriented for the (220) Bragg reflection. The incident wavelength of our neutron beam is 1.054 A° and φ_o the straight-through beam angle is 341.5°. The spectrometer was hand operated.

For preliminary orientation of our crystal we used a gun-sight mount consisting of a rotatable table which can also be tilted through an angle of about 45°.

The crystal itself is cylindrical in shape with a length of about 3.25 cm. and a diameter of 1.6 cm. We found a (110) plane 30° off the cylindrical axis so a suitable crystal mount was designed to hold the (110) plane vertical. This enabled all (hhl) reflections to be seen simply by rotating the crystal. (See Fig.4).

An electric furnace designed and built by Stephen Boronkay is used for this project. The furnace can maintain temperatures from 350° C to 800° C or more with temperature variations less than ± 1/10 of a degree. A controlled temperature change of between 5 and 10° C can be effected in a matter of 4 or 5 minutes, after which time the temperature fluctuations are less than $\pm \frac{1}{2}^{\circ}$ C. (See Fig.5).

The furnace is water-cooled by means of copper-tubing around four equally spaced flanges at the base of the furnace through which various thermocouple junctions pass to its centre. Three concentric layers of thin steel cylinders help prevent radiation losses. The outer steel casing of the furnace is 1/4" thick except at the height of the neutron beam where the thickness is pared to 1/8".

To prevent heat conduction the crystal is mounted on a thin ceramic rod projecting vertically from the centre of the base of the furnace.

Attached to the furnace is a diffusion pump and Pirani gauge. The furnace heaters are automatically shut off by a relay if the pressure inside the furnace rises above 0.02 torr. The relay also has a high temperature trip and a low-cooling-water flow trip to further protect the furnace heaters.

The furnace has three heaters: 30-watt heaters at top and bottom, each of which is controlled by a variable transformer, and a 1500-watt cage-type heater which is connected to the temperature controller and a variable transformer. The temperature controller varies the main heater power by means of a Silicon Controlled Rectifier whose controlling input comes from a thermocouple located in the furnace midway between the sample and the heater coils. A base thermocouple input voltage is selected on a digital dial setting connected to the controller. The chosen thermocouple voltage is maintained by proportional power variation. This means that the difference between the actual heater output and the base heater output is proportional to the difference between the actual thermocouple voltage and the base thermocouple voltage. (See Fig.6)

Thermocouple reference junctions were maintained at 0° C. through the use of a Zeref automatic ice-point unit.

EXPERIMENTAL WORK

The crystal was initially found to be in the disordered state. An ordering process consisting of the following steps was carried out. The temperature was raised to 535° C. (~ 20° above Tc) for 10 hours. Next, the temperature was lowered to 500° C. for 4 hours. Finally it was successively decreased in temperature intervals of 10 degrees for periods doubling in length for each change until a temperature of 460° C. was reached. The duration of the process was 60 hours.

Integrated intensity measurements of the (100) and (200) Bragg peaks indicated that the crystal was approximately 30% ± 15% ordered at the end of the above process.

The crystal was mounted in the furnace and oriented on the spectrometer. The (100) reflection was obtained and the temperature in the furnace was raised to 502° C. at which point the decrease of intensity with time was measured. (See Figs. 7 and 8). It was found that the time constant for disordering, τ , was 4.0 ± 1.0 minutes. The large error results from the nearness of the temperature to T_c (515 ± 5° C.) and the associated short relaxation time for the disordering process. It is worth noting that our neutron statistics are good enough to enable measurement of such a short time constant.

The crystal was re-ordered at 460° C. and (since a paper by Litvin, Udovenko and Vintaikin, 1971, cited this as the fastest ordering temperature) some measurements of superlattice peak intensity were recorded. The data was insufficient for a graphical display but an approximate ordering time constant of 35 ± 10 hours was obtained.

Upon completion of this reordering process, Ψ- rocking curves were obtained for (100), (200) and (300) planes of the crystal. (See Figs. 9, 10, 11). The (100) peak was very broad, having a half-width, Γ , of 2.2 degrees. The (200) peak had a half-width of 1.4 degrees and its peak intensity was seven times larger than that of the (100) reflection. The ratio of the measured integrated intensities however, was close to one, which indicated a higher degree of order in the crystal than had previously been obtained. The true order parameter was substantially less than one when the effect of extinction was accounted for. Nonetheless, this is of minor importance for it is not the exact degree of order which is of interest to us, but the rate of change of order.

The reordered system was allowed to come to equilibrium at 480° C. before the temperature was suddenly raised to 487° C. Thermal fluctuations of crystal temperature dissipated after 6 minutes and (100) Bragg peak measurements were recorded as a function of time. A plot of intensity versus time was made on a linear scale from which we deduced the equilibrium intensity after 18 hours. (See Fig. 12).

On a semi-logarithmic scale a plot of (initial minus equilibrium) intensity versus time was constructed. (See Fig. 13). The experimental points fall (within error) on a straight line from whose slope is deduced an order relaxation time constant, τ , of 39.0 ± 2.0 minutes at a temperature of 487° C.

DISCUSSION

Order relaxation time constants have been measured for two temperatures near T_c. As the temperature is decreased below T_c the time constant of disordering increases in magnitude. It is seen that the time constants will be long in comparison with the thermal equilibration time of the furnace and the time for a neutron measurement but still short enough to be easily measured. Thus the feasibility of the final experiment has been demonstrated.

There remains only the collection of sufficient data for measurement of the critical exponent of relaxation time for long-range order.

LIST OF FIGURES

Fig.1 Typical bcc structure showing order-disorder effects for an alloy AB.

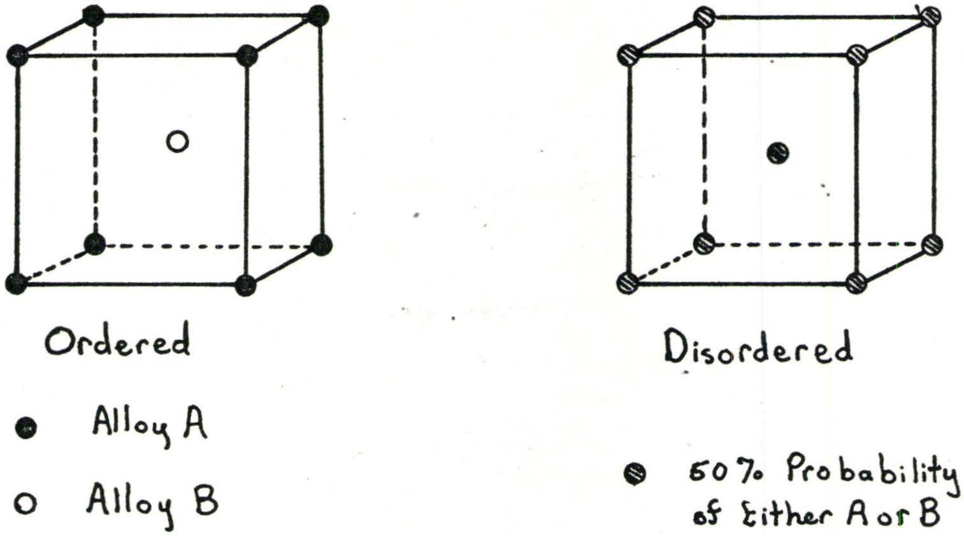

Fig. 2. Sketch showing how the position of the jth atom within the unit cell is specified by $\underline{r}_j = u_j\underline{a} + v_j\underline{b} + w_j\underline{c}$ where u_j, v_j, w_j are constants

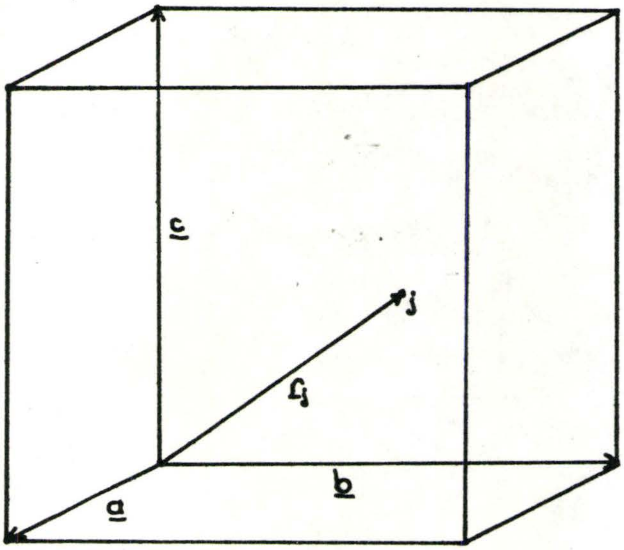

Fig. 3. Schematic diagram of 2-axis spectrometer

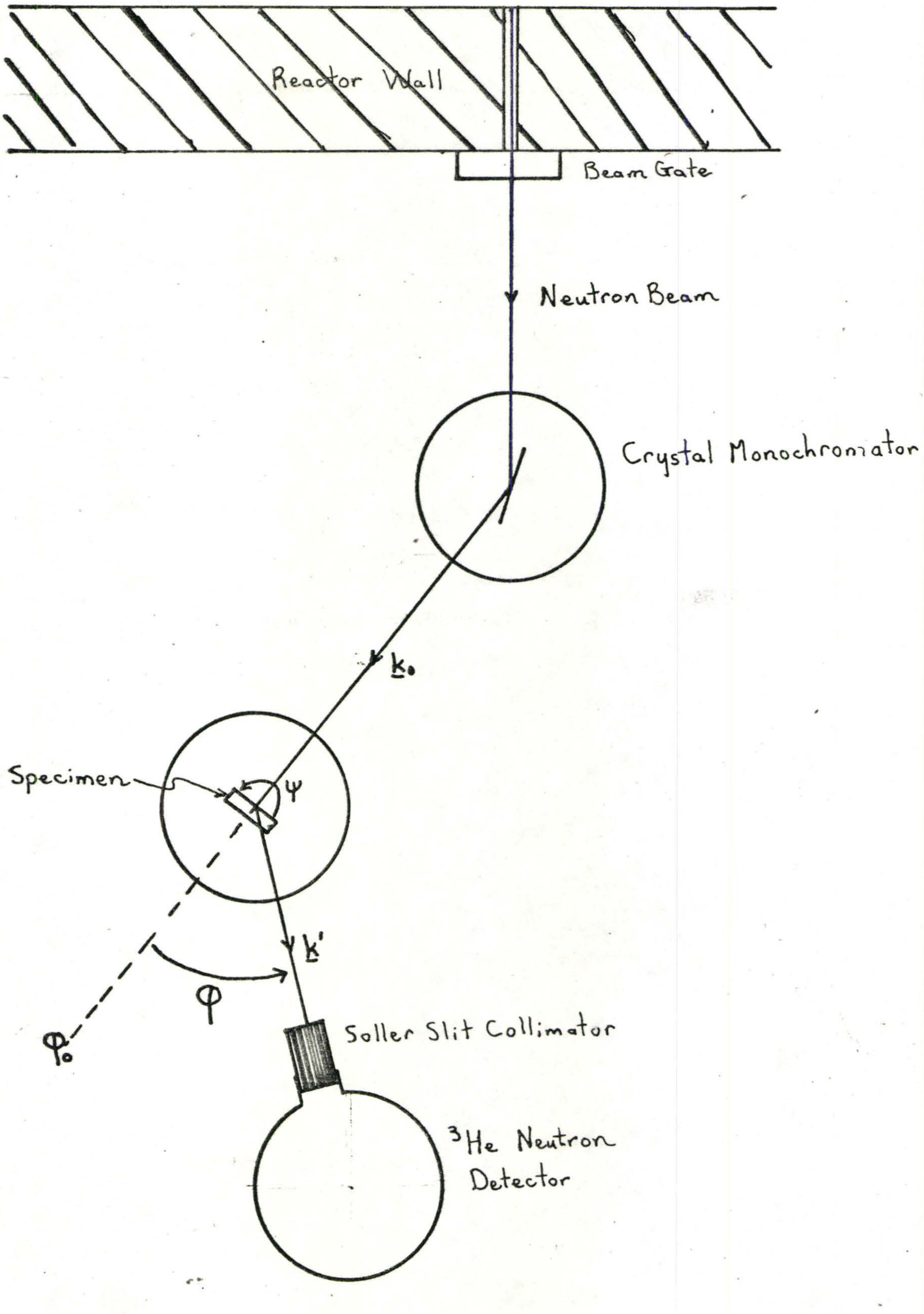

Fig. 4 Side View of Final Crystal Mount (Actual Size)

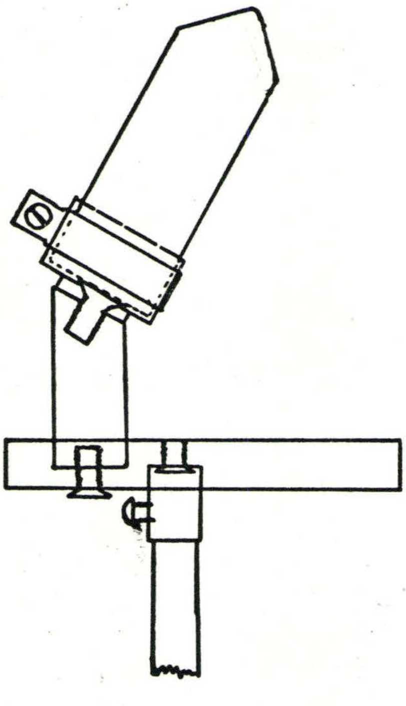

Fig. 5 Schematic plot abstracted from actual data showing crystal temperature versus time for our electric furnace showing approach to equilibrium for a 6 degree temperature change.

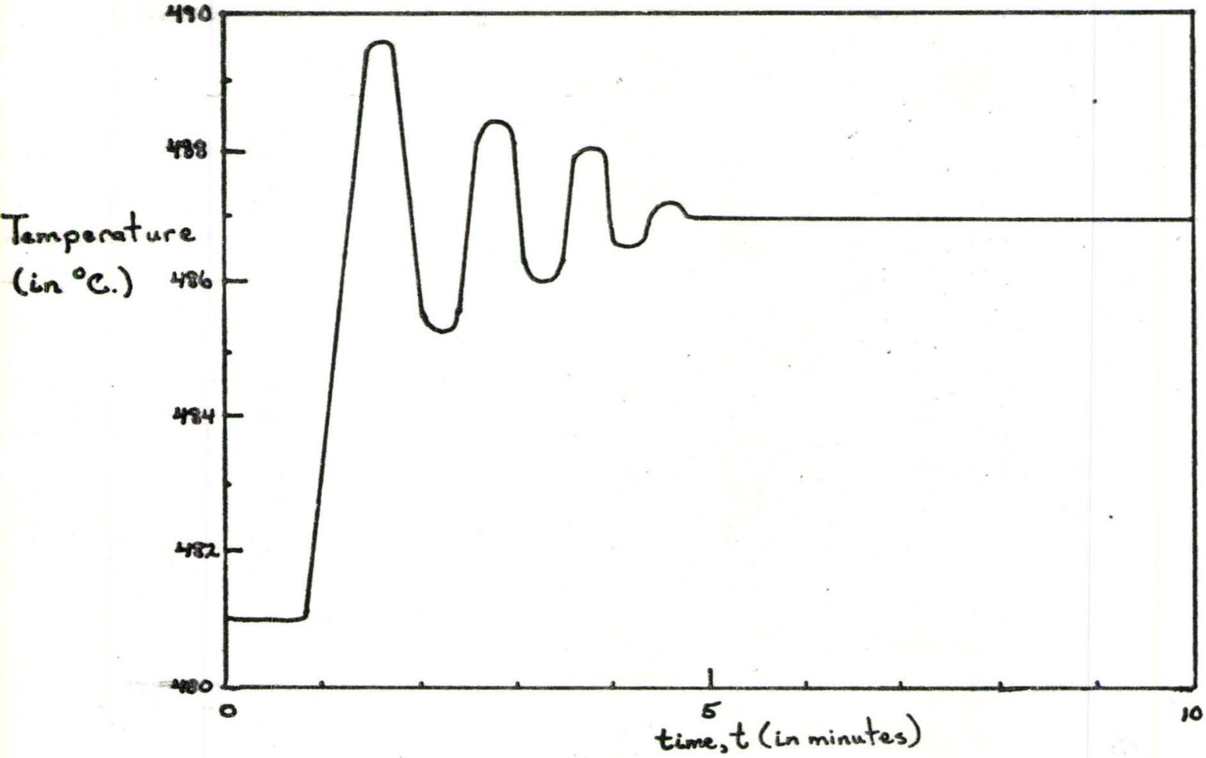

Fig. 6. Corresponding plots of thermocouple input voltage and power versus time for the furnace temperature controller (Schematic)

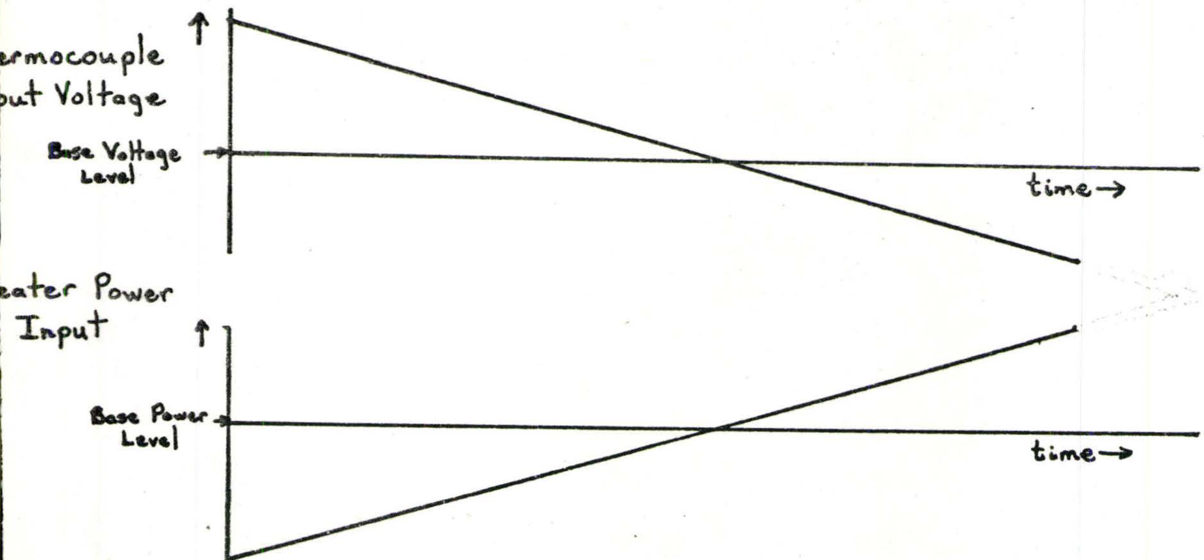

Fig.7 Plot of Intensity versus time for (100) Bragg peak of Ni_3Mn showing order relaxation at 502°C.

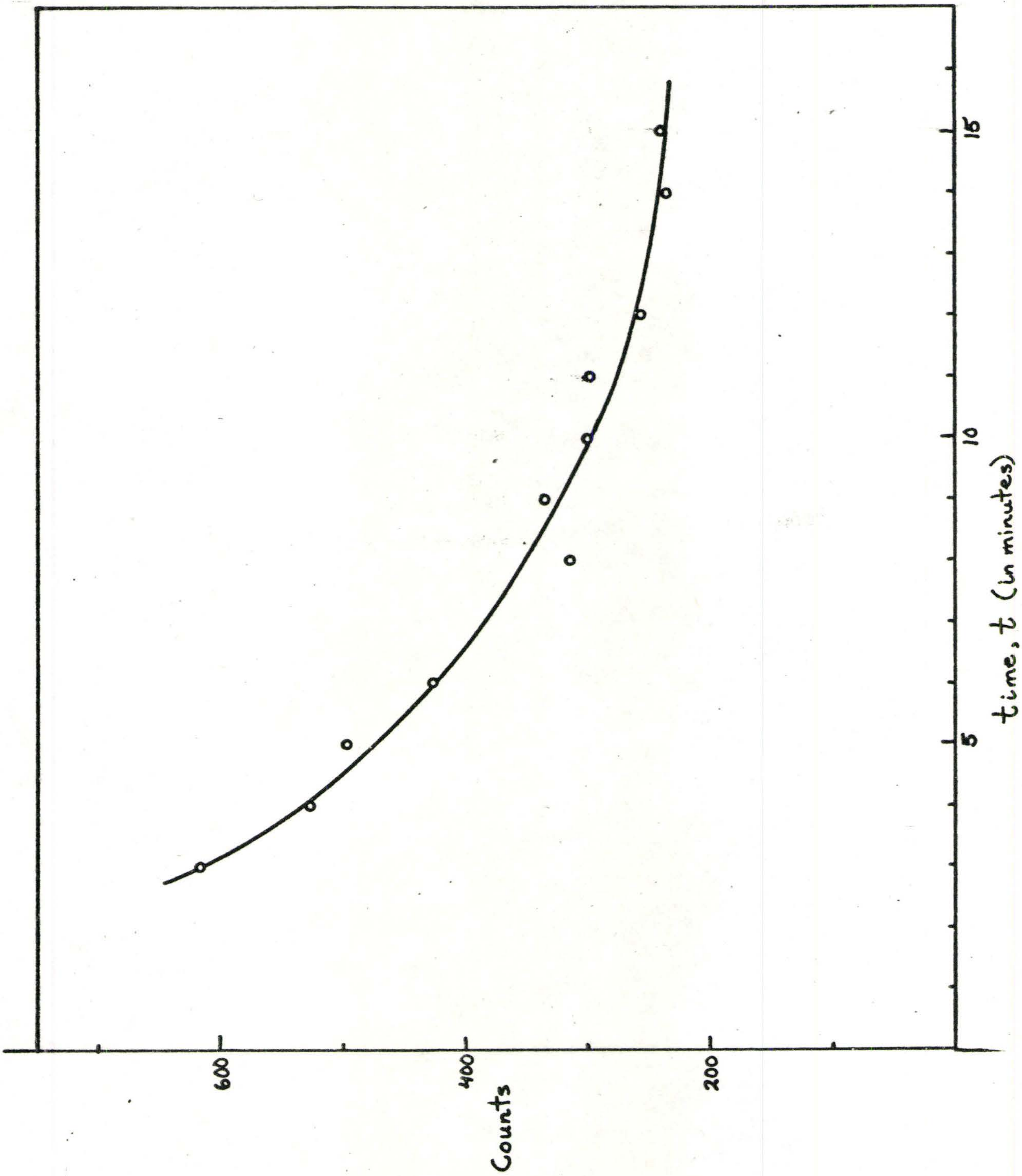

Fig. 8 Semi-log plot of (100) peak intensity minus equilibrium intensity versus time for Ni_3Mn at 502°C.

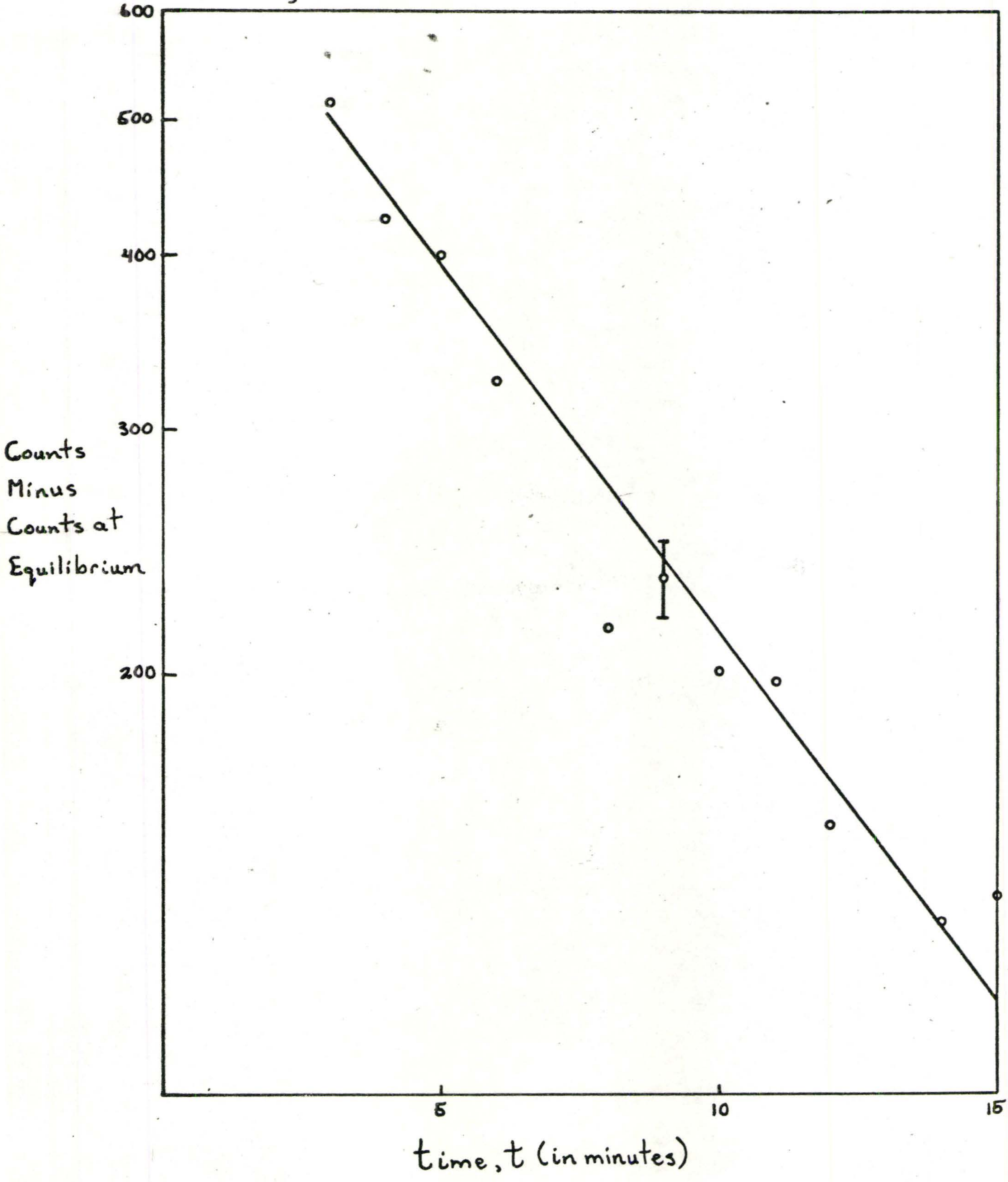

Fig. 9 (100) Ψ-Rocking Curve for Ni_3Mn (460°C.)

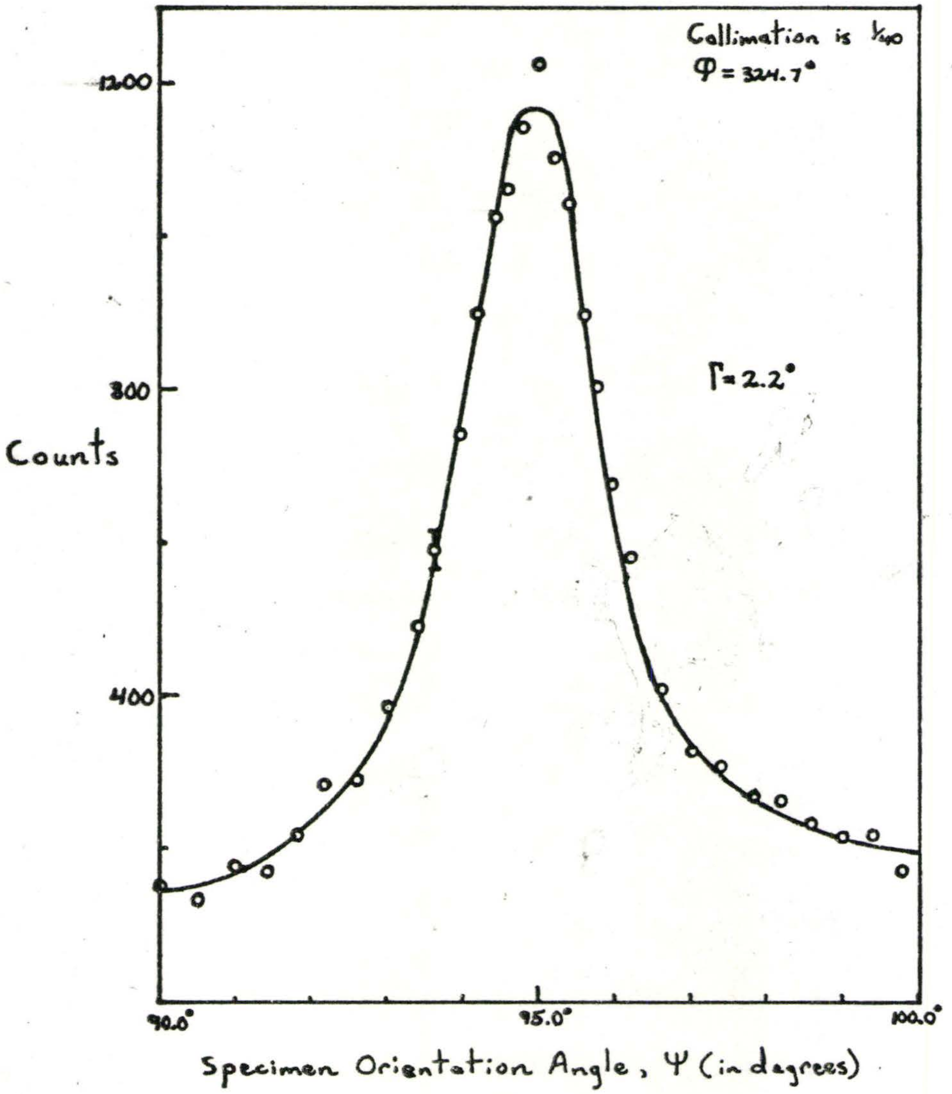

Fig. 10 (200) Ψ-Rocking Curve for Ni_3Mn

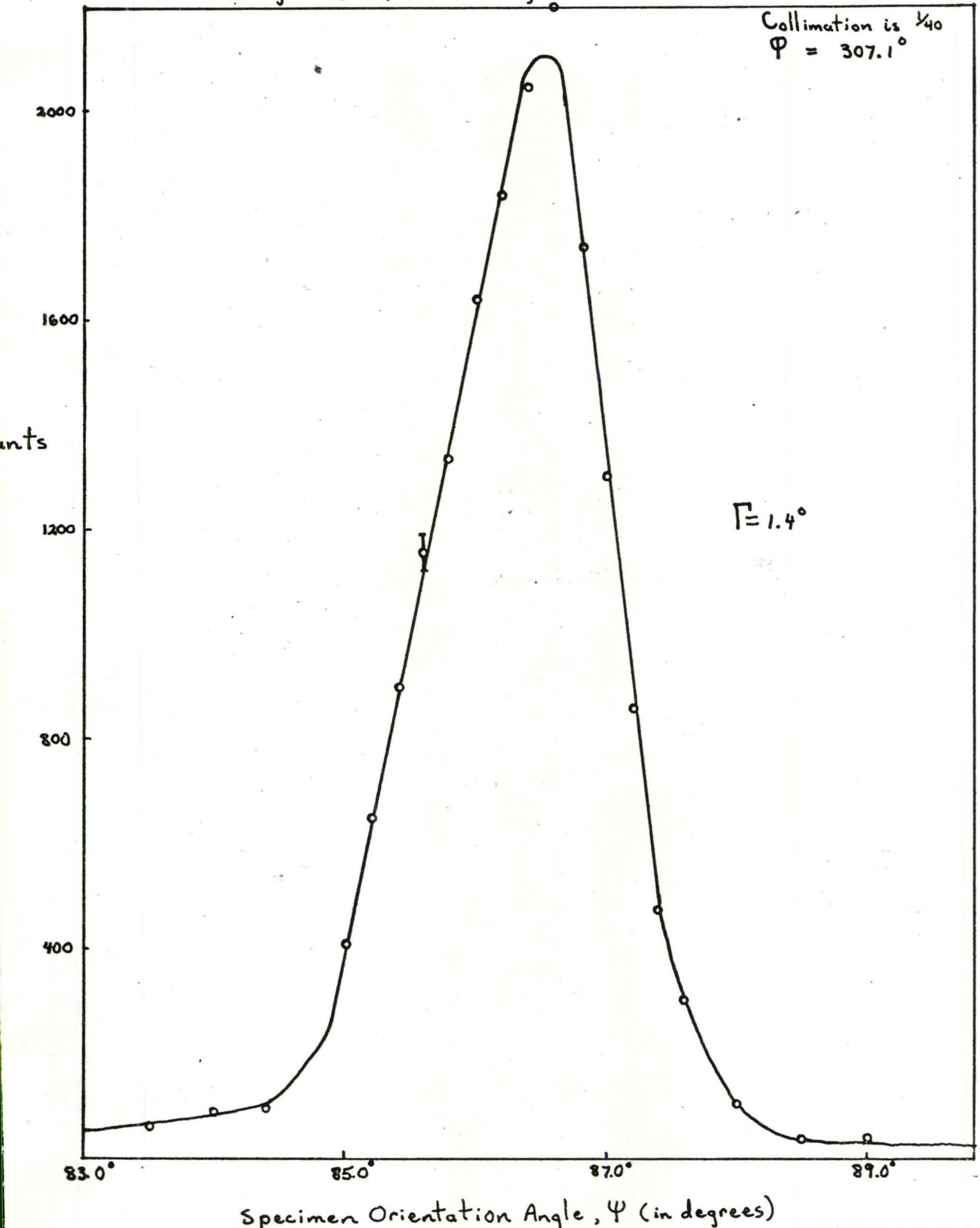

Fig. 11 (300) Ψ - Rocking Curve for Ni_3Mn (460°C.)

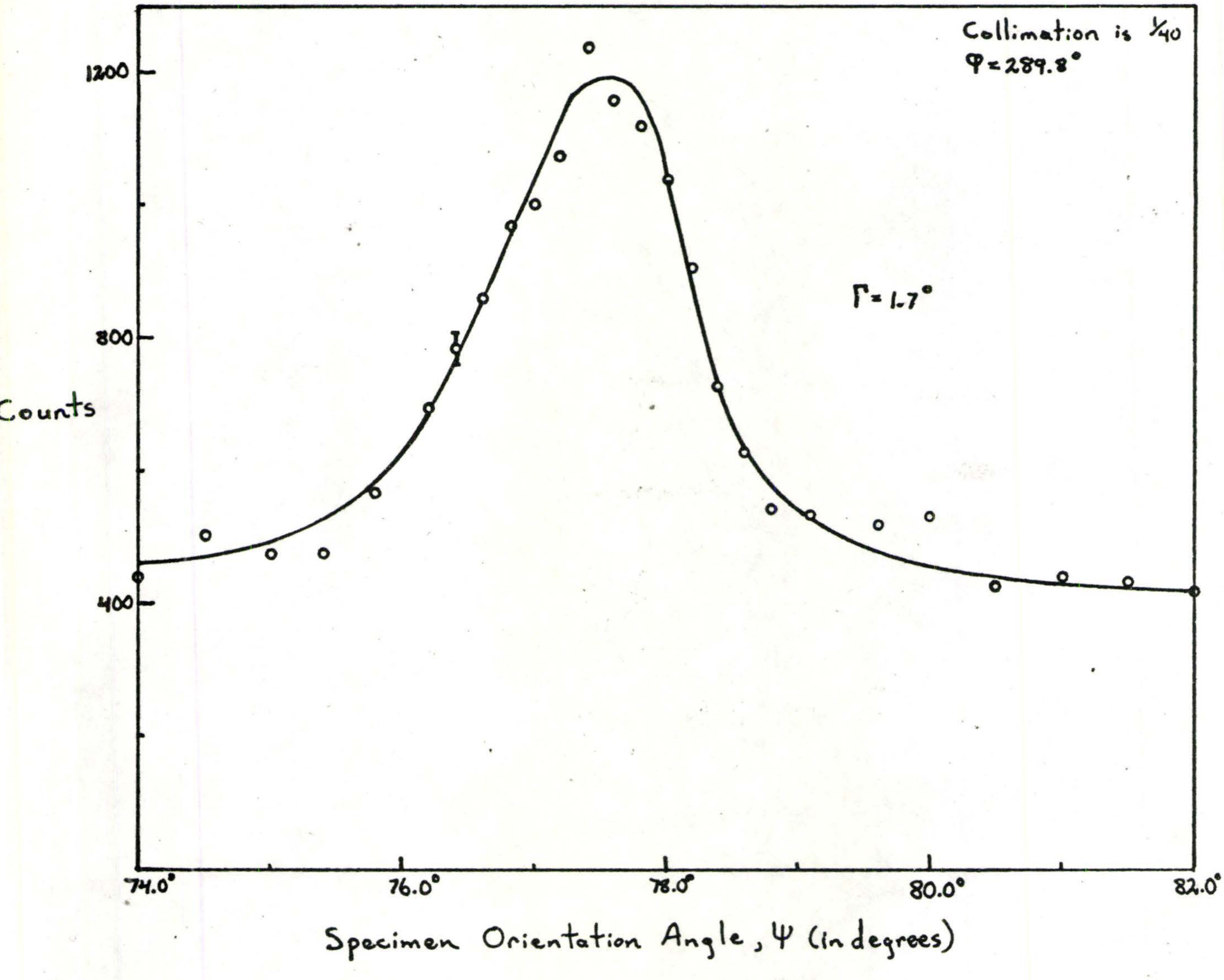

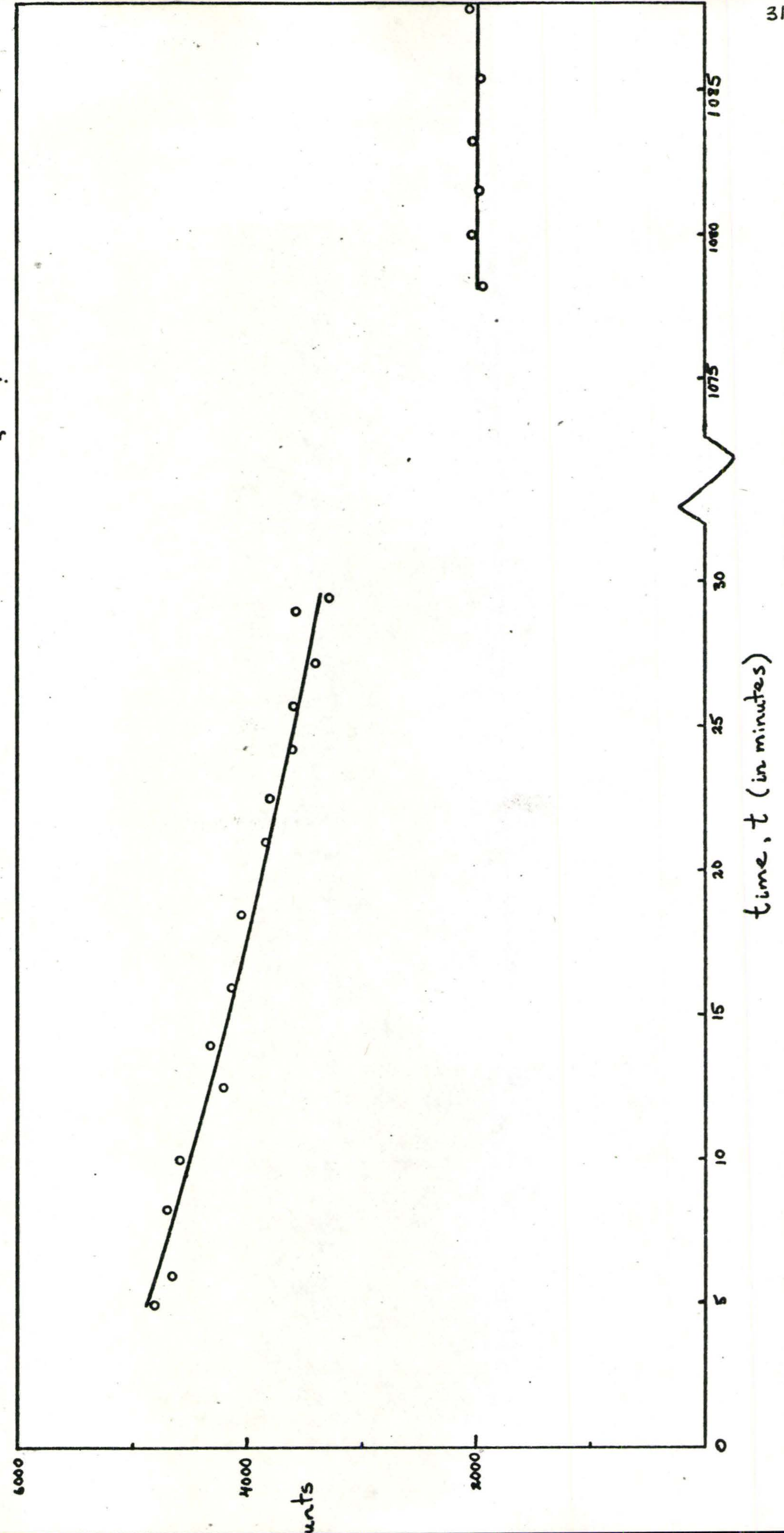

Fig. 12 Plot of Intensity versus time for (100) Bragg peak after a sudden temperature change from 480°C to 487°C. The crystal is Ni_3Mn. The curve shows order relaxation at 487°C.

Fig. 13. Semi-log plot of (100) peak intensity minus equilibrium intensity versus time for Ni_3Mn at 487°C.

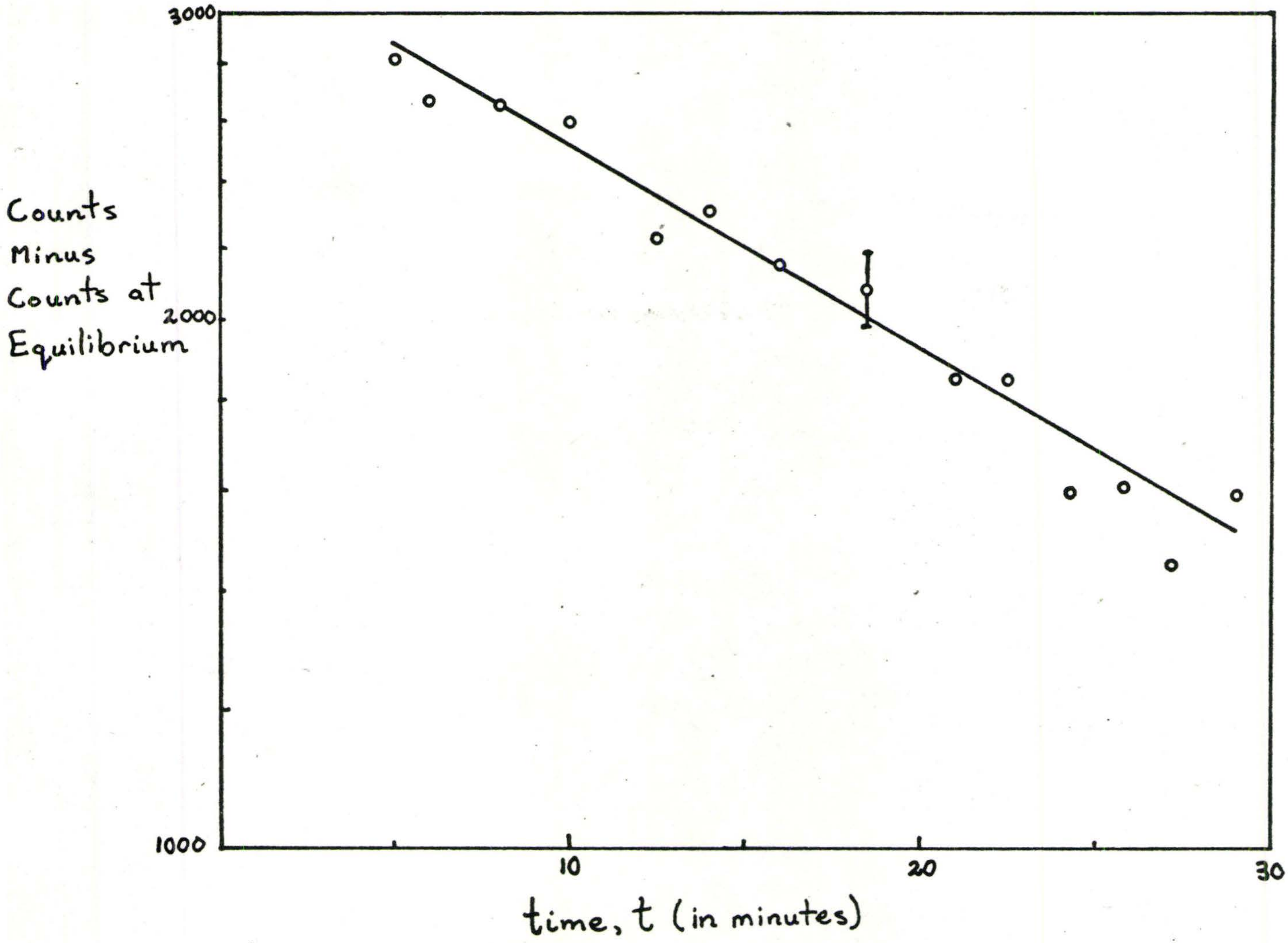

REFERENCES

1. G.E. Bacon, Neutron Diffraction, 2nd Ed., Clarendon Press, Oxford, 1962.
2. L. Guttman, Solid State Physics, Vol. 3, Academic Press, New York, 1956
3. W.C. Hamilton, Acta. Cryst. 10 (1957) 629
4. K. Huang, Statistical Mechanics, Wiley, New York, 1963
5. C. Kittel, Introduction to Solid State Physics, 3rd Ed., Wiley, New York, 1966
6. D.F. Litvin, V.A. Udovenko and E.Z. Vintaikin, Soviet Physics - Doklady 16 (1971) 486
7. N. Ogita, A. Ueda, T. Matsubara, H. Matsuda and F. Yonezawa, J. Phys. Soc. Japan, 26 Supplement (1969) 145
8. C.G. Shull and S. Siegel, Phys. Rev. 75 (1949) 1008
9. H. Yahata, J. Phys. Soc. Japan, 30 (1971) 657

BIBLIOGRAPHY

1. L.R. Aronin, J. Appl. Phys. 23 (1952) 642
2. G.E. Bacon, Neutron Diffraction, 2nd Ed., Clarendon Press, Oxford, 1962
3. L. Guttman, Solid State Physics, Vol. 3, Academic Press, New York, 1956
4. W.C. Hamilton, Acta. Cryst. 10 (1957) 629
5. K. Huang, Statistical Mechanics, Wiley, New York, 1963
6. C. Kittel, Intro. to Solid State Physics, 3rd Ed., Wiley, New York, 1966
7. D.F. Litvin, V.A. Udovenko, E.Z. Vintaikin, Soviet Physics - Doklady 16 (1971) 486
8. J.C. Norvell and J. Als-Nielsen, Phys. Rev. B 2 (1970) 277
9. G.R. Piercy and E.R. Morgan, Can. J.Phys. 31 (1953) 529
10. N. Ogita, A. Ueda, T. Matsubara, H. Matsuda and F. Yonezawa, J. Phys. Soc. Japan, 26 Supplement (1969) 145
11. C.G. Shull and S. Siegel, Phys. Rev. 75 (1949) 1008
12. C.G. Shull and M.K. Wilkinson, Phys. Rev. 97 (1955) 304
13. H.E. Stanley, Introduction to Phase Transitions and Critical Phenomena, Clarendon Press, Oxford, 1971
14. H. Yahata, J. Phys. Soc. Japan 30 (1971) 657